

# Mechanistic Studies of Catalytic Carbon–Carbon Cross-Coupling by Well-Defined Iron NHC Complexes

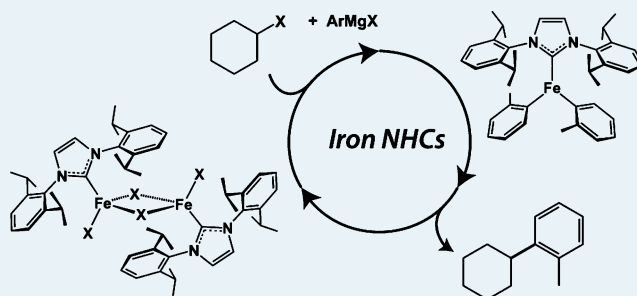
Jacob A. Przyowski, Kevin P. Veggeberg, Hadi D. Arman, and Zachary J. Tonzetich\*

Department of Chemistry, University of Texas at San Antonio, San Antonio, Texas 78249, United States

**S** Supporting Information

**ABSTRACT:** The mechanism of iron-catalyzed carbon–carbon cross-coupling reactions between Grignard reagents and alkyl halides has been investigated using well-defined N-heterocyclic carbene (NHC) compounds. The iron(II) precatalyst,  $[\text{Fe}_2\text{Cl}_2(\mu\text{-Cl})_2(\text{IPr})_2]$ , was employed in several C–C cross coupling reactions exhibiting the ability to efficiently couple primary and secondary alkyl halides with several aryl and alkyl Grignard reagents. For selected substrates, a 2 mol % catalyst loading (4 mol % Fe) afforded conversions of >99% and were achieved with <8% homocoupling of the electrophile. The mechanism of the coupling reaction was studied by means of radical clock, radical trap, and single-turnover experiments, which support a radical-based cycle involving an Fe(II/III) redox couple. The implications of this mechanism on the efficacy of iron-NHC-catalyzed cross-coupling reactions are discussed.

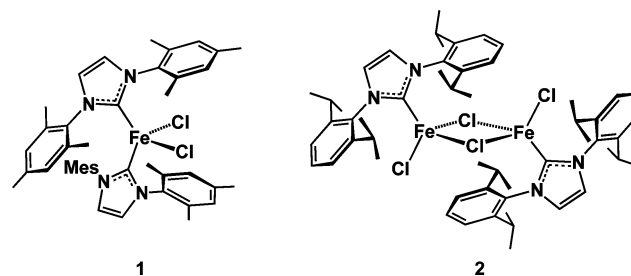
**KEYWORDS:** iron catalysis, cross-coupling, radical mechanisms, N-heterocyclic carbenes, three-coordinate complexes

**INTRODUCTION**

The progression toward earth-abundant catalysts as an alternative to precious metals has recently garnered significant attention. This change of focus has ushered iron into the forefront of research for its environmental compatibility and broad availability.<sup>1,2</sup> Recently, there has been particular interest in N-heterocyclic carbene (NHC)-containing systems.<sup>3–5</sup> Iron compounds employing NHC ligands have shown the ability to facilitate a variety of reactions, including biaryl cross-coupling,<sup>6–8</sup> alkyl–alkyl cross-coupling,<sup>9</sup> alkyl–aryl cross-coupling,<sup>10–15</sup> arylmagnesium,<sup>16</sup> aldehyde esterification,<sup>17</sup> alkyne trimerization,<sup>18</sup> allylic substitution,<sup>19–22</sup> and hydro-silylation.<sup>23–30</sup>

A growing library of NHC-supported iron compounds have been synthesized and characterized, forming a strong foundation for efforts in rational catalyst design with earth-abundant transition metals.<sup>31–42</sup> A variety of carbenes have been employed in an effort to effectively modulate the steric and electronic properties of the resulting catalysts.<sup>30,43–45</sup> The stoichiometric reactivity and redox chemistry of these compounds have been scrutinized to provide a connection between the nature of the ligand and the observed catalytic efficacy. Our laboratory has been focusing on the iron chemistry of the ubiquitous aryl-substituted NHC ligands (Chart 1). In previous work, we have reported straightforward synthetic routes to halide complexes of both iron(II) and iron(III) containing the IMes and IPr NHC ligands.<sup>46</sup> We envisioned that such species would serve as well-defined precatalysts for Kumada-type cross-couplings and afford us the

Chart 1. IMes and IPr Complexes of Iron(II)



opportunity to examine the mechanism of such reactions in detail.

Although there are now several examples of iron-NHC-catalyzed cross-coupling reactions, no consistent mechanistic picture has emerged. In work using binary mixtures of IMes and  $\text{Fe}(\text{OAc})_2$ , Cardenas demonstrated evidence for an iron(I/III) couple via single-electron steps.<sup>9</sup> Using alkyl-substituted NHCs, Deng and co-workers described clean coupling to alkyl halides with both phenyl and alkynyl complexes of the type  $[\text{Fe}(\text{R})_2(\text{NHC})_2]$ .<sup>47,48</sup> In this system, it was also demonstrated that coupling proceeded through a pathway involving carbon-based radicals. With other supporting ligands, such as chelating phosphines, in-depth studies by Nakamura and Neidig have pointed to an iron(II/III)-based mechanism,<sup>15,49–51</sup> and work

Received: July 10, 2015

Revised: August 27, 2015

Published: August 28, 2015

by Bedford has demonstrated a possible role for iron(I).<sup>52–55</sup> Studies by Hu et al. with a pincer-ligated iron system have also shown strong support for a radical-based iron(II/III) mechanism,<sup>56</sup> although the geometric and electronic requirements of the anionic pincer ligand are likely very different from those of simple neutral donors, such as phosphines and NHCs.

In addition to these examples with well-defined complexes, the mechanisms of cross-coupling reactions with iron catalysts that lack strongly coordinating ligands have also been examined.<sup>57–63</sup> Studies with such “ligand free” systems have also demonstrated evidence for carbon-based radicals in the catalytic cycle, although the reaction pathways appear to be dependent upon the nature of the electrophile.<sup>64</sup>

Despite these important contributions, the scope of mechanistic information concerning C–C cross-coupling by iron is still relatively small. The nature of the supporting ligands appears to play a large role, and the noted shortcomings of iron-catalyzed cross-coupling reactions such as electrophile homocoupling and limited substrate scope are not always accounted for by the various reported mechanisms. We were therefore eager to exploit the well-defined nature of certain aryl-substituted NHC-iron systems to investigate the mechanism of Kumada-type cross-coupling reactions.

## RESULTS AND DISCUSSION

**Catalytic Trials.** Complexes **1** and **2** were screened for catalytic activity in cross-coupling reactions using a variety of alkyl/aryl halides and Grignard reagents. Testing several different substrate combinations demonstrated little to no catalytic activity for complex **1**. Thus, a focus was placed on the reactivity of complex **2**. Underlying reasons for the lower efficacy of **1** versus **2** are not known at this time, although we speculate that an increase in coordination number for catalytic intermediates derived from **1**, which feature a 2:1 NHC to Fe stoichiometry, may attenuate activity. The results of representative catalytic trials employing **2** are presented in Table 1. The most successful substrate pairings for reactions catalyzed by **2**

**Table 1.** Kumada-Type Cross-Coupling Reactions Employing **2** As Precatalyst<sup>a</sup>

entry	electrophile	RMgCl	conversion <sup>b</sup> (%)	yield <sup>c</sup> (%)
1	CyCl	Ph	99	54
2	CyBr	Ph	96	83
3	CyI	Ph	87	78
4	CyBr	Bn	99	87
5	CyBr	<i>n</i> -hexyl	71	28
6	CyBr	<i>i</i> -Pr	N.D.	0
7	CyBr	HC≡C	0	0
8	1-bromooctane	Ph	95	71
9	1-bromooctane	Bn	93	11
10	1-bromooctane	<i>n</i> -hexyl	93	2
11	<i>t</i> -BuBr	Ph	N.D.	6
12	4-bromotoluene	Ph	59	2
13	4-iodotoluene	Ph	57	1

<sup>a</sup>Reactions conditions: 1 equiv of electrophile, 1.1 equiv of RMgCl, 2 mol % **2**, THF solvent, stirred under N<sub>2</sub> from –30 °C to RT over 1 h.

<sup>b</sup>Consumption of electrophile as determined by GC/MS against an eicosane internal standard. <sup>c</sup>Amount of cross-coupled product as determined by GC/MS against an eicosane internal standard.

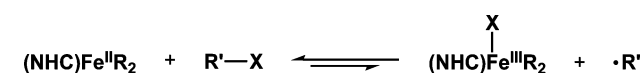
comprised alkyl electrophiles and aryl nucleophiles. In the case of cyclohexyl halides (CyX), chlorides, bromides, and iodides all underwent cross-coupling successfully with phenyl Grignard, although yields for CyCl were slightly lower than those for CyBr and CyI (Table 1, entries 1–3). Productive alkyl–alkyl cross-coupling was also observed for selected Grignard reagents; however, these reactions were very sensitive to the nature of the nucleophile. Benzyl Grignard was tolerated well, but significantly reduced yields were obtained upon switching to *n*-hexylMgCl or *i*-PrMgCl. These results suggest that nucleophiles containing β-hydrogen atoms are poor coupling partners with the iron-NHC catalyst system. Although lacking β-hydrogen atoms, ethynyl Grignard also proved unsuitable as a nucleophile in cross-coupling reactions with CyBr (Table 1, entry 7). The small nature of the ethynyl group likely leads to an unstable iron alkyl species resulting in rapid catalyst deactivation. This premise is consistent with the apparent stability of three-coordinate iron(II) dialkyl complexes discussed below.

Coupling of the primary alkyl electrophile 1-bromooctane with PhMgCl was comparable to analogous reactions with CyBr; however, much lower yields were obtained when benzyl and *n*-hexyl Grignard were employed as nucleophiles (Table 1, entries 8–10). Conversion remained high in these instances, suggesting that unproductive reactivity of the electrophile was hampering catalytic turnover. In line with this idea, electrophile homocoupling was observed to increase significantly in reactions with 1-bromooctane and alkyl Grignard reagents.

In contrast to primary and secondary alkyl halides, both tertiary alkyl halides and aryl halides were observed to be very poor substrates in cross-coupling reactions. Very little cross-coupled product was detected in reactions with PhMgCl (Table 1, entries 11–13). In both cases, the expected products of electrophile homocoupling were not observed in significant quantities.

Although variations of iron-catalyzed cross-coupling reactions have been reported to utilize a range of coupling partners, the largest numbers of successful coupling reactions make use of alkyl electrophiles, in agreement with the results obtained from our catalytic trials.<sup>10,12,13,65–70</sup> The preference for alkyl electrophiles over aryl electrophiles in these reactions is most consistent with an electrophile activation step that proceeds via a radical process (halogen atom abstraction, Scheme 1), as

**Scheme 1.** Halogen Atom Abstraction from a Carbon Electrophile by Iron(II)

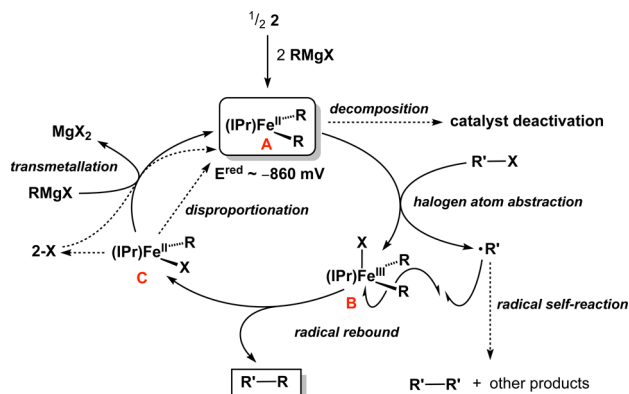


opposed to concerted oxidative addition. This notion is further supported by numerous reports that demonstrate the intermediacy of alkyl radicals in the iron-catalyzed cross-coupling reactions mentioned above. Moreover, halogen atom abstraction by high-spin iron(II) has a direct parallel in the initiation step of atom-transfer radical polymerization, in which this process is now a well-established pathway for alkyl halides.<sup>71–73</sup>

Additional evidence for a radical-based mechanism in the IPr-Fe catalyst system was garnered from experiments in the presence of radical inhibitors. For the case of CyBr and PhMgCl, addition of BHT (2,6-di-*tert*-butyl-4-methylphenol) completely prevented the formation of the phenylcyclohexane

product. Furthermore, when coupling reactions between CyBr and *n*-hexylMgCl were performed in toluene, small quantities of benzylcyclohexane were detected. We ascribe the formation of benzylcyclohexane to the coupling of cyclohexyl and benzyl radicals, the latter of which are generated by H atom abstraction from solvent by the cyclohexyl radical. On the basis of these considerations and the findings of several other research groups,<sup>50,51,56</sup> we favor a mechanistic proposal for iron-catalyzed C–C cross-coupling that involves a radical-based iron(II/III) cycle (Scheme 2). This mechanism is consistent

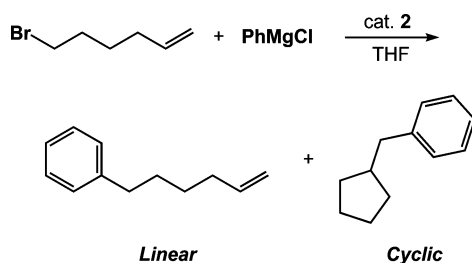
**Scheme 2. Proposed Catalytic Cycle for Cross-Coupling by the IPr-Fe Catalyst System**



with the preference for alkyl over aryl electrophiles and can also account for the presence of both electrophile homocoupling and H atom abstraction via indiscriminate reactivity of the electrophile radical ( $R'^{\bullet}$ ). This mechanistic scenario also avoids invoking exotic oxidation states for the iron catalyst, which are not well corroborated by electrochemical measurements (*vide infra*).

**Behavior of Electrophile Radicals.** To probe the mechanism in Scheme 2 further, we next carried out a series of experiments with the radical clock electrophile, 1-bromo-5-hexene. The radical formed at the 1-position of this substrate is capable of undergoing cyclization to the cyclopentylmethyl radical. We elected to use PhMgCl as the nucleophile in these reactions because it provides the best results with the related 1-bromooctane. As expected, reactions between 1-bromo-5-hexene and PhMgCl catalyzed by **2** produced a mixture of the cyclized and uncyclized coupling products indicative of the presence of electrophile radicals (Scheme 3). The appearance alone of both of these products, however, does not address the question of whether the electrophile radical remains solvent-caged with the catalyst during turnover. To resolve this issue,

**Scheme 3. Possible Products Resulting from Coupling of 1-Bromo-5-hexene and PhMgCl**



we next examined the effect of increasing the catalyst loading on the ratio of linear (uncyclized) to cyclized product (Figure 1). As depicted in Figure 1, the linear product was found to

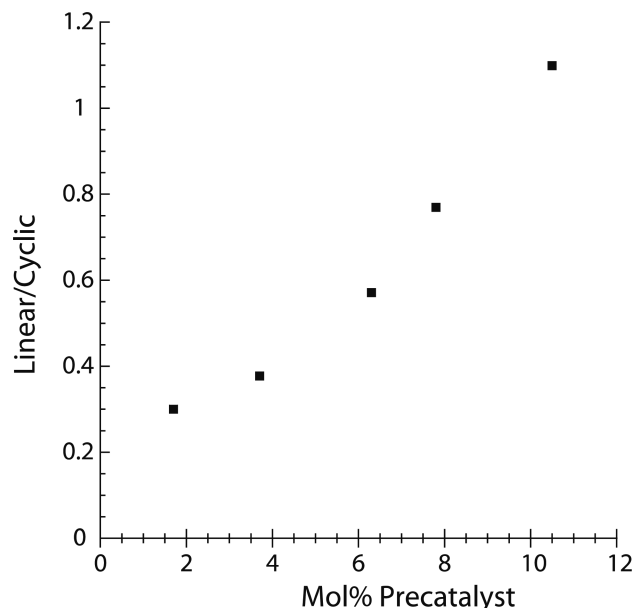


**Figure 1.** Ratio of 5-hexenylbenzene (linear product) to (cyclopentylmethyl)benzene (cyclic product) as a function of catalyst loading in the reaction of 1-bromo-5-hexene (0.28 M) with PhMgCl catalyzed by **2** in THF.

increase as a function of catalyst loading. This behavior is consistent with electrophile radical dissociation from the solvent cage of the catalyst. Higher catalyst loadings lead to an increased concentration of the iron(III) species depicted in Scheme 2 (B), resulting in a higher probability of collisions with the electrophile radical prior to cyclization. The amount of cyclization for a solvent-caged electrophile radical would be expected to show no dependence on catalyst loading because the recombination event is effectively zero-order in catalyst concentration.<sup>56</sup>

To further address the issue of electrophile radical reactivity, we next performed a series of experiments designed to probe the propensity for electrophile homocoupling at different overall reaction concentrations. The CyBr/*n*-OctMgCl system was selected for these experiments because it produced a measurable amount of electrophile homocoupling that was conveniently assayed by GC/MS. The results of these experiments are shown in Figure 2 and demonstrate that an increased ratio of homocoupled-to-cross-coupled product is obtained at higher reaction concentrations. Such a result is once again consistent with dissociation of electrophile radicals from the solvent cage of the catalyst. Increasing the concentration of CyBr without a concomitant increase in catalyst loading should result in a greater number of self-collisions between cyclohexyl radicals over recombination with catalyst molecules.<sup>74</sup> This trend is consistent with the mechanistic framework in Scheme 2 and the findings of the radical clock experiments.

**Iron Alkyl Complexes.** Alkyl and aryl complexes of iron NHCs can be envisioned to serve as models for intermediate species in iron-catalyzed cross-coupling schemes and are therefore of great value to mechanistic studies. Despite this fact, only a small sample of hydrocarbyl complexes of iron(II) have been synthesized that contain aryl-substituted NHC

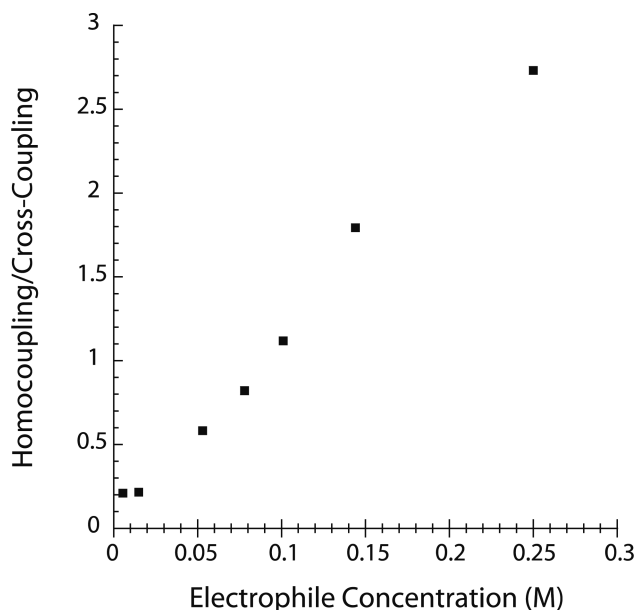
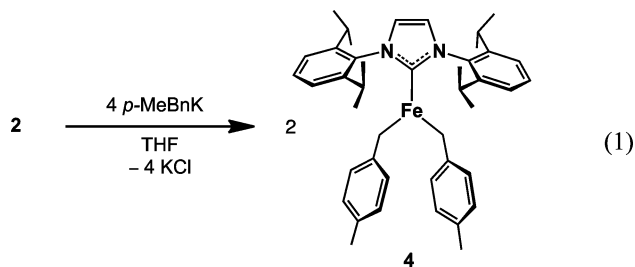


**Figure 2.** Ratio of bicyclohexane (homocoupled) to octylcyclohexane (cross-coupled) as a function of electrophile concentration in the reaction of CyBr with *n*-OctMgCl catalyzed by 2 mol % of **2** in THF.

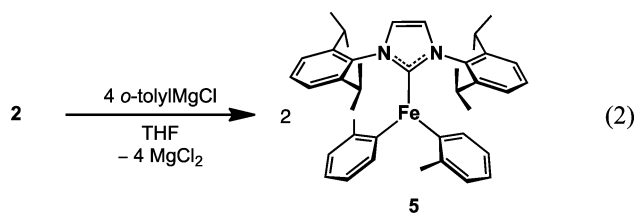
ligands. These compounds include the three-coordinate  $[\text{Fe}(\text{R})_2(\text{IPr})]$  species ( $\text{R} = \text{Bn}$ , **3**;  $\text{CH}_2\text{SiMe}_3$ , **6**; and mesityl), and the four-coordinate complex,  $[\text{Fe}(\text{CH}_3)_2(\text{IMes})_2]$ .<sup>27,37,75</sup> To expand upon the number of such compounds and provide a means of comparing the stoichiometric reactivity of different hydrocarbyl groups, we have prepared two new three-coordinate  $[\text{Fe}(\text{R})_2(\text{IPr})]$  complexes.

Treatment of **2** with 4 equiv of *p*-MeBnK in THF afforded the three-coordinate dityl complex, **4** eq 1. Complex **4**



demonstrates NMR features very comparable to those of **3** with the exception of a new singlet resonance at +75.6 ppm attributable to the Me group of the *p*-xylyl ligand (see Supporting Information).

In addition to **4**, we have also prepared an example of an iron aryl complex by reaction of **2** with four equiv of *o*-tolylMgCl eq 2. Complex **5** is a rare example of a three-coordinate iron(II)



diaryl. Similar reactions of **2** with PhMgCl and MesMgBr led only to intractable mixtures. Much like **3** and **4**, compound **5**

displays a very diagnostic  $^1\text{H}$  NMR spectrum in benzene- $d_6$ , with paramagnetically shifted peaks observable for each of the *o*-tolyl hydrogen atoms (see Supporting Information). The complex was also subjected to an X-ray diffraction study, and the structure solution is depicted in Figure 3. The metric

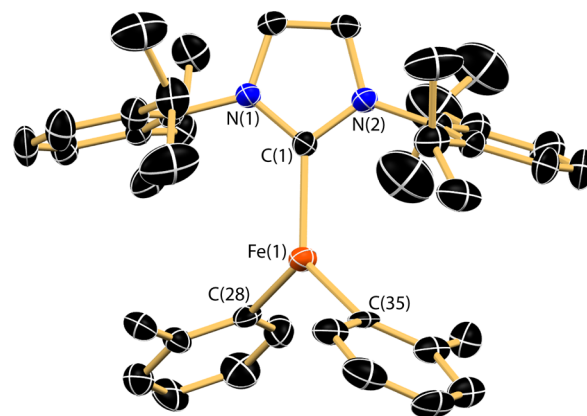


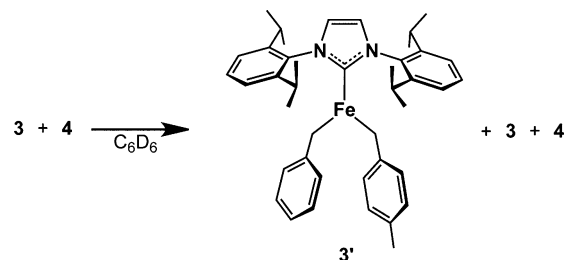
**Figure 3.** Solid-state structure of  $[\text{Fe}(\textit{o}\text{-tolyl})_2(\text{IPr})]$  (**5**). Hydrogen atoms and minor components of the disordered aryl rings omitted for clarity. Selected bond distances and angles can be found in the Supporting Information.

parameters about iron in **5** are comparable to those published for **3**, **6**, and  $[\text{Fe}(\text{Mes})_2(\text{IPr})]$ , with a slight elongation of the  $\text{Fe}-\text{C}_{\text{aryl}}$  bond distances (avg. of  $\text{Fe}(1)-\text{C}(28)$  and  $\text{Fe}(1)-\text{C}(35) = 2.121(3) \text{ \AA}$ ).<sup>37,75,76</sup>

One outstanding issue in iron-catalyzed cross-coupling concerns the nature of the turnover-limiting species. Several groups have proposed that peralkylated anionic iron species, so-called “ate” complexes, may account for the majority of iron in the presence of excess carbon nucleophile (i.e., Grignard reagents).<sup>55,56</sup> In certain instances, such hypotheses are supported by kinetic data.<sup>77</sup> Given our ability to isolate well-defined hydrocarbyl complexes, we next investigated their behavior in the presence of one another and upon addition of exogenous Grignard.

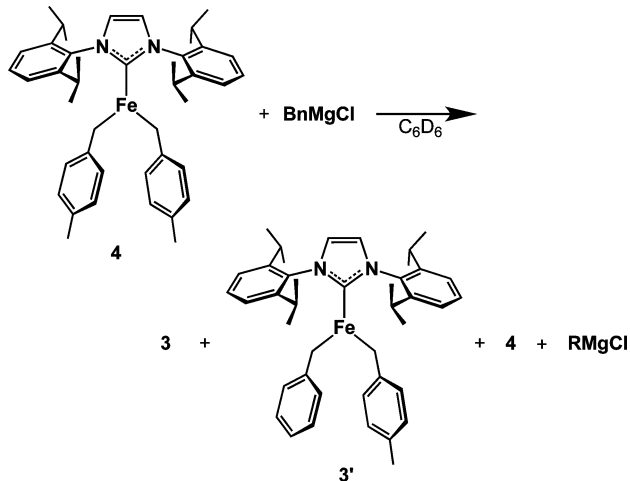
Binary mixtures of complexes **3**–**5** in benzene- $d_6$  were generated and subjected to  $^1\text{H}$  NMR spectroscopy (see Supporting Information). The spectra demonstrated that scrambling of the alkyl ligands occurred readily for combinations of both **3** and **4**, and **3** and **5**, producing mixtures of all possible  $[\text{Fe}(\text{R})_2(\text{IPr})]$  species. In the case of **3** and **4**, the steric and electronic properties of the hydrocarbyl ligands are nearly identical, leading to a purely statistical 1:2:1 distribution of **3**/**3'**/**4** for stoichiometric mixtures (Scheme 4). In similar fashion, addition of one equivalent of BnMgCl to **4** led to exchange of

#### Scheme 4. Alkyl Ligand Scrambling Behavior between **3** and **4** in Solution



alkyl ligands and production of a mixture of  $[\text{Fe}(\text{R})_2(\text{IPr})]$  species (Scheme 5). In this case, a 1:2:2 ratio of 3/3'/4 was observed, again indicating a statistical distribution of all possible dialkyls.

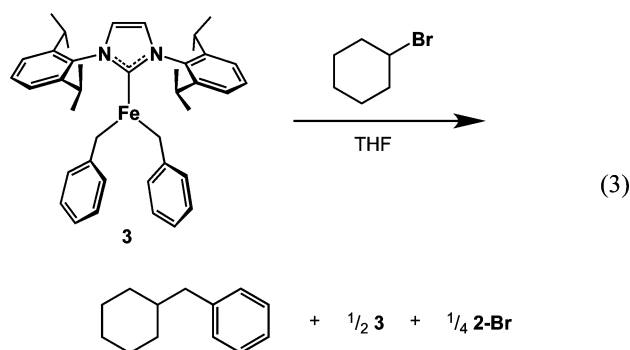
**Scheme 5.** Alkyl Ligand Scrambling Behavior between 4 and  $\text{BnMgCl}$  in Solution



The results of experiments with 3–5 are consistent with three-coordinate iron(II) NHC complexes that are dynamic in solution, undergoing constant exchange of alkyl ligands between iron centers and Grignard reagents. The nature of this exchange process is not known at this time, but we favor a pathway involving bimetallic species featuring bridging hydrocarbyl ligands.<sup>7,78</sup> Whether such behavior also occurs for more coordinatively saturated four-coordinate iron alkyls is uncertain. Of note, however, Danopoulos and Braunstein did report the synthesis of the three-coordinate monoalkyl compound,  $[\text{FeCl}(\text{CH}_2\text{SiMe}_3)(\text{IPr})]$ ,<sup>37</sup> which is stable toward disproportionation. The stability of this compound may be a function of the bulky  $\text{CH}_2\text{SiMe}_3$  ligand that effectively slows bimolecular reactivity between iron centers. We have also observed sluggish reactivity with 6 in experiments with alkyl bromides (vide infra).

**Stoichiometric Reactions.** Compounds 3–6 were next subjected to stoichiometric reactions with the prototypical carbon electrophile,  $\text{CyBr}$ , to determine if three-coordinate iron(II) bis(hydrocarbyl) species are chemically competent in the cross-coupling reaction. Complexes 3–5 reacted cleanly with  $\text{CyBr}$  at room temperature to afford the desired cross-coupled products as judged by GC/MS. In contrast, no coupled product was detected in stoichiometric reactions involving 6. The lack of reactivity with 6 is most likely a function of the substantial steric bulk of the trimethylsilylmethyl groups, which may occlude access to the iron center. Such sluggish reactivity is also consistent with the reported stability of  $[\text{FeCl}(\text{CH}_2\text{SiMe}_3)(\text{IPr})]$  toward disproportionation.

The iron-containing products resulting from reaction of  $[\text{Fe}(\text{R})_2(\text{IPr})]$  with  $\text{CyBr}$  were scrutinized for the case of 3. The  $^1\text{H}$  NMR spectrum of the reaction components in benzene- $d_6$  after removal of THF indicated a mixture of 3 and the dimeric bridging bromide species, 2-Br. This observation can be accounted for by the limiting stoichiometry depicted in eq 3. Such a scenario is consistent with comproportionation of a monobenzyl species,  $[\text{FeBr}(\text{CH}_2\text{Ph})(\text{IPr})]$ , resulting from cross-coupling of one of the two benzyl



ligands. No other iron-containing byproducts were detected by NMR spectroscopy indicating that  $[\text{Fe}(\text{R})_2(\text{IPr})]$  species are chemically competent in C–C cross-coupling and capable of regenerating species that lie on the catalytic cycle depicted in Scheme 2.

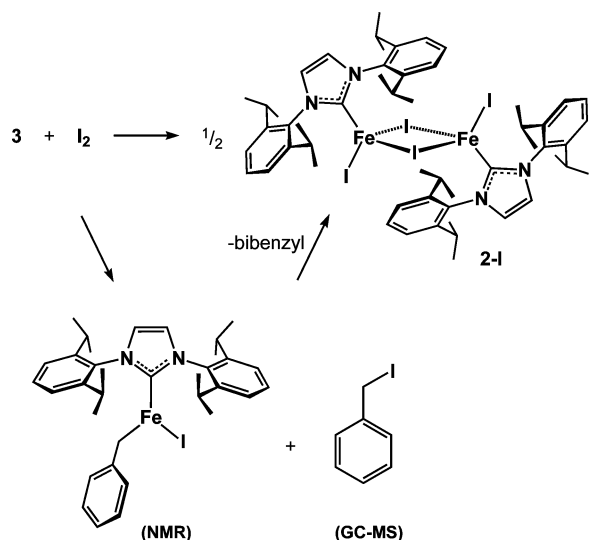
On the basis of the clean reactivity of complexes 3–5 with electrophiles, we next tested the relative propensity for coupling to aryl versus benzyl nucleophiles by conducting a competition experiment between 3 and 5 with  $\text{CyBr}$ . As stated above, 3 and 5 react with one another prior to addition of electrophile to produce a statistical mixture of different iron hydrocarbyls. Nonetheless, we surmised that such reactivity would not prevent us from determining which hydrocarbyl group (benzyl vs *o*-tolyl) would couple more effectively with  $\text{CyBr}$  because all possible species are present in solution. An analysis of the product mixture by GC/MS demonstrated that nearly all coupling had occurred to the *o*-tolyl group (~98%). Therefore, we conclude that the observed superiority of aryl Grignard reagents over benzyl and alkyl Grignard reagents in cross-coupling reactions catalyzed by 2 (vide supra) is due to the greater propensity for iron aryls to undergo C–C bond formation with electrophile radicals. The more efficient rebound in these cases may be a function of the reduced steric congestion about the Fe–C bond afforded by the  $\text{sp}^2$ -hybridized carbon centers.

As a final set of experiments, we examined the redox activity of the dibenzyl complex, 3. The cyclic voltammogram of 3 was recorded in THF at a glassy carbon electrode (see Supporting Information). The complex was found to display an irreversible anode event at  $-0.864$  V versus the ferrocene/ferrocenium couple, consistent with oxidation to iron(III). This low potential demonstrates the potent reducing ability of  $[\text{Fe}(\text{R})_2(\text{IPr})]$  complexes and further supports their role as the key species in electrophile activation. In an attempt to prepare the iron(III) species resulting from halogen atom abstraction, we investigated the reaction of 3 with  $\text{I}_2$ . Mixing 3 and 1 equiv of  $\text{I}_2$  in benzene- $d_6$  produced bibenzyl and the iodide-bridged iron(II) species,  $[\text{Fe}_2\text{I}_2(\mu\text{-I})_2(\text{IPr})_2]$  (2-I) as judged by  $^1\text{H}$  NMR. Crystals of 2-I were obtained from the reaction mixture and subjected to X-ray diffraction, confirming the identity of the iron species as the bridged diiodide complex (see Supporting Information).

Our inability to isolate an iron(III) alkyl complex was not unexpected, given the instability of such species toward reduction. Deng has reported that one-electron oxidation of four-coordinate  $[\text{FePh}_2(\text{IPr}_2\text{Me}_2)_2]$  by  $(\text{Cp}_2\text{Fe})(\text{BPh}_4)$  leads to facile reductive elimination of biphenyl and production of reduced iron compounds.<sup>47</sup> That result supports the hypothesis that concerted reductive elimination from an iron(III) species can account for the C–C bond formation event during iron-

catalyzed cross-coupling. Reductive elimination from iron(III) during cross-coupling would require that the electrophile radical add to an iron(II) molecule. Such a scenario differs from the mechanistic framework outlined in Scheme 2, where C–C bond formation occurs through a radical rebound process to iron(III). In our IPr-Fe system, the isolation of **2-I** from the reaction of **3** with I<sub>2</sub> does not rule out concerted reductive elimination as a means of producing bibenzyl because the resulting iron(I) species could be captured by iodine to regenerate iron(II); however, we have also examined the reaction of **3** with a substoichiometric amount of I<sub>2</sub> (~0.5 equiv). This experiment demonstrated that benzyl iodide was formed along with a new iron complex that we tentatively assign as the monobenzyl species, [FeI(CH<sub>2</sub>Ph)(IPr)], on the basis of its <sup>1</sup>H NMR spectrum (see Supporting Information). The appearance of benzyl iodide and [FeI(CH<sub>2</sub>Ph)(IPr)] argues against concerted reductive elimination in favor of a process involving discrete steps, as outlined in Scheme 6. The

Scheme 6. Reaction of **3** with I<sub>2</sub>



reactions in Scheme 6 are compatible with the overall mechanism displayed in Scheme 2, where bibenzyl would be formed through subsequent halogen atom abstraction of benzyl iodide by [FeI(CH<sub>2</sub>Ph)(IPr)] or **3** and radical rebound to form the new C–C bond.

**Mechanistic Picture.** Taken together, the observations with the IPr-Fe system discussed here are most consistent with the mechanistic hypothesis displayed in Scheme 2. The proposed active species is a three-coordinate iron(II) hydrocarbyl complex (**A**) that forms by transmetalation of the precatalyst with RMgX. We cannot say with certainty that a dihydrocarbyl species is required for halogen atom abstraction, given that an iron(II) monohydrocarbyl monohalide species may be equally reactive toward this process;<sup>79</sup> however, attempts to isolate a monobenzyl or monoaryl species with the IPr ligand were not successful.

The stability of the hydrocarbyl complex also appears to be critical. Its inability to form or its propensity toward rapid decomposition can account for the observed lack of reactivity with certain nucleophiles (Table 1, entries 6 and 7) and with precatalyst **1**. Nonetheless, there is no requirement that the nucleophile be a Grignard reagent, only that it be capable of effecting transmetalation to iron(II).<sup>80</sup> To demonstrate this

point, we have examined the catalytic reaction between CyBr and both diphenylzinc and *p*-MeBnK. Employing precatalyst **2**, both reactions were found to yield the cross-coupled product in high yields comparable to those of PhMgCl and BnMgCl.

Once **A** is formed, it is capable of abstracting a halogen atom from the electrophile to generate a radical (R<sup>•</sup>) and the iron(III) species, [FeX(R)<sub>2</sub>(IPr)] (**B**). At this point, the electrophile radical dissociates from the solvent cage containing **B** and can rebound with **B** or react with any **A** that has not undergone halogen atom abstraction. We favor a pathway involving rebound to complex **B** for the following reasons: Formation of an iron(III) trialkyl species by addition of R<sup>•</sup> to **A** should result in significant quantities of nucleophile homocoupling. The lack of appreciable nucleophile homocoupling in reactions catalyzed by **2** is notable, especially in the case of reactions between CyBr and PhMgCl, in which a large amount of biphenyl would be expected because of the kinetic favorability of aryl–aryl reductive elimination over alkyl–aryl. Mechanisms have also been put forth that avoid concerted reductive elimination by invoking a direct reaction of the electrophile radical with **A**.<sup>51</sup> The result of radical rebound to **A** then generates an iron(I) complex that is proposed to disproportionate with **B** to regenerate iron(II). We believe this scenario to be unlikely, given the large excess of electrophile present that should sequester any iron(I) formed, leaving the fate of the iron(III) complex unresolved. Furthermore, DFT calculations performed on compound **6** do not show significant spin-density on the alkyl ligands, arguing against their direct involvement in a radical rebound process.<sup>76</sup>

The precise nature of the rebound process between the electrophile radical and **B** is not known at this time. Neither do we have any direct evidence for the structure of **B**. However, our data do demonstrate some important characteristics: First, the rebound process appears to be more rapid with aryl nucleophiles than with alkyl nucleophiles, which accounts for their superior performance in cross-coupling reactions. This observation is consistent with both the catalytic trials and the competition experiments with complexes **3** and **5**. Second, the amount of electrophile homocoupling is observed to increase with alkyl versus aryl nucleophiles. This result can be rationalized by positing that slow rebound of R<sup>•</sup> to the alkyl group bound to **B** results in a longer-lived electrophile radical that is subject to self-reaction. Third, increasing the overall electrophile concentration leads to increased electrophile homocoupling as the self-reaction of R<sup>•</sup> becomes more likely than rebound to **B**.

## CONCLUSIONS

The mechanism of catalytic cross-coupling by iron complexes containing N-heterocyclic carbene ligands has been investigated. As a result of our studies, we draw the following conclusions concerning the behavior and catalytic activity of three-coordinate iron NHC catalysts in cross-coupling reactions:

- (1) Cross-coupling reactions catalyzed by iron NHC complexes proceed via a radical-based mechanism involving halogen atom abstraction from the carbon electrophile.
- (2) Three-coordinate iron(II) dihydrocarbyl complexes are chemically competent in cross-coupling reactions involving alkyl halides.

- (3) Complexes of the form  $[\text{Fe}(\text{R})_2(\text{IPr})]$  readily undergo facile ligand exchange in solution with other iron complexes and Grignard reagents but remain neutral three-coordinate species.
- (4) The extent of electrophile homocoupling is largely determined by the nature of the carbon nucleophile. The propensity for electrophile radical recombination with the metal-bound nucleophile follows the order aryl > benzyl > *n*-alkyl.
- (5) Nucleophiles other than Grignard reagents are successful coupling partners so long as they are capable of effectively transmetallating to iron(II).

As a final note, we recognize that the particular mechanisms of cross-coupling reactions catalyzed by iron may be highly subject to the nature of ligands, coordination number, and spin state.<sup>81</sup> Therefore, although the findings presented here are in agreement with several other studies involving similar catalyst systems, we are hesitant to suggest that a unified mechanism exists for iron-catalyzed cross-coupling.<sup>82</sup>

## EXPERIMENTAL SECTION

**General Comments.** All manipulations were performed in a Vacuum Atmospheres glovebox under an atmosphere of purified nitrogen. Tetrahydrofuran, diethyl ether, pentane, and toluene were purified by sparging with argon and passage through two columns packed with 4 Å molecular sieves. Benzene-*d*<sub>6</sub> was dried over sodium and vacuum-distilled prior to use. <sup>1</sup>H NMR spectra were recorded on a Varian Inova spectrometer operating at 500 MHz (<sup>1</sup>H) and referenced to the residual protium resonance of the solvent at 7.16 ppm relative to tetramethylsilane. Because of the paramagnetism of each compound, the peak multiplicities of all observable NMR resonances were singlets and are not explicitly denoted below. GC/MS was performed on an Agilent 6890N. Cyclic voltammetry was performed at 23 °C on a CH Instruments 620D electrochemical workstation. A three-electrode setup was employed comprising a platinum working electrode, platinum wire auxiliary electrode, and a Ag/AgCl quasi-reference electrode. Triply recrystallized Bu<sub>4</sub>NPF<sub>6</sub> was used as the supporting electrolyte. All electrochemical data were referenced externally to the ferrocene/ferrocenium couple at 0.00 V. Analytical data were obtained from the CENTC Elemental Analysis Facility at the University of Rochester.

**Materials.**  $[\text{FeCl}_2(\text{IMes})_2]$ ,  $[\text{Fe}_2\text{Cl}_2(\mu\text{-Cl})_2(\text{IPr})_2]$ , and  $[\text{Fe}(\text{CH}_2\text{SiMe}_3)_2(\text{IPr})]$  were prepared according to literature procedures.<sup>46,76</sup>  $[\text{Fe}(\text{CH}_2\text{Ph})_2(\text{IPr})]$  was prepared according to a modification of the published procedure and is reproduced below for convenience. *p*-MeBnK was synthesized by a method analogous to that of BnK.<sup>83,84</sup> All Grignard reagents were purchased from commercial suppliers and used as received. All alkyl halides were purchased from commercial suppliers, sparged with nitrogen, and stored over 4 Å molecular sieves prior to use.

**X-ray Data Collection and Structure Solution Refinement.** Crystals of **5** and **2-I** suitable for X-ray diffraction were mounted in Paratone oil onto a glass fiber and frozen under a nitrogen cold stream maintained by an X-Stream low-temperature apparatus. The data were collected at 98(2) K using a Rigaku AFC12/Saturn 724 CCD fitted with Mo *K*<sub>α</sub> radiation ( $\lambda = 0.71073$  Å). Data collection and unit cell refinement were performed using Crystal Clear software.<sup>85</sup> Data processing and absorption correction giving minimum and

maximum transmission factors were accomplished with Crystal Clear and ABSCOR,<sup>86</sup> respectively. All structures were solved by direct methods and refined on *F*<sup>2</sup> using full-matrix, least-squares techniques with SHELXL-97.<sup>87,88</sup> All non-hydrogen atoms were refined with anisotropic displacement parameters. All carbon-bound hydrogen atom positions were determined by geometry and refined by a riding model. Crystallographic data and refinement parameters can be found in the Supporting Information.

**General Procedure for Catalytic Reactions.** Catalytic trials were performed using a 6.8 mM stock solution of precatalyst **2** in THF. Into a 20 mL scintillation vial, 339 μmol of electrophile and 339 μmol of eicosane (as internal standard) were added to 1.00 mL of the precatalyst stock solution. The resulting solution was chilled to −30 °C, at which point 375 μmol of the Grignard reagent was added. The reaction mixture was allowed to stir for 1 h, during which time it warmed to ambient temperature (~23 °C). After this time, the solution was quenched with 5 mL of a concentrated oxalic acid solution. The organic-soluble materials were extracted into 10 mL of diethyl ether, diluted, and subjected to GC/MS analysis. For all coupling reactions, control experiments were performed in the absence of **2** to ensure no background reactivity of the electrophile with the Grignard reagent.

**Stoichiometric Cross-Coupling Reactions.** A solution of iron dialkyl (**3–5**) was prepared in THF. To the stirring solution was added 1 mol equiv of cyclohexyl bromide. The solution was stirred at RT for 1 h prior to being quenched with 5 mL of a concentrated oxalic acid solution. The organic-soluble materials were extracted into 10 mL of diethyl ether and subjected to GC/MS analysis.

**$[\text{Fe}(\text{CH}_2\text{Ph})_2(\text{IPr})]$ , **3**.** A round-bottom flask was charged with 352 mg (342 μmol) of  $[\text{Fe}_2\text{Cl}_2(\mu\text{-Cl})_2(\text{IPr})_2]$  and 15 mL of diethyl ether. The resulting suspension was frozen at −196 °C. To the thawing/stirring suspension was added 1.24 mL (1.37 mmol) of BnMgCl as a 1.10 M solution in 2-MeTHF. The mixture was allowed to stir for 2 h at ambient temperature. After this time, the orange suspension was filtered through a plug of Celite to remove the insoluble magnesium salts. The resulting orange solution was concentrated in vacuo and chilled to −30 °C for 24 h. During this time, the desired compound precipitated as 311 mg (72% yield) of orange crystals. NMR parameters matched those published previously.<sup>37</sup> <sup>1</sup>H NMR:  $\delta$  21.42 (2 carbene-CH), 20.83 (4 CHMe<sub>2</sub>), 19.53 (4 *m*-Ar<sup>IPr</sup>H), 11.38 (2 *p*-Ar<sup>IPr</sup>H), −6.13 (12 CHMe<sub>2</sub>), −20.4 (br, 12 CHMe<sub>2</sub>), −43.4 (br, 4 *o*/*m*-Ar<sup>Bn</sup>H), −77.6 (br, 4 *o*/*m*-Ar<sup>Bn</sup>H), −88.60 (2 *p*-Ar<sup>Bn</sup>H).

**$[\text{Fe}(\text{CH}_2\text{-}p\text{-tolyl})_2(\text{IPr})]$ , **4**.** A round-bottom flask was charged with 207 mg (201 μmol) of  $[\text{Fe}_2\text{Cl}_2(\mu\text{-Cl})_2(\text{IPr})_2]$  and 15 mL of diethyl ether. To the stirring suspension was added 115 mg (804 μmol) of *p*-MeBnK. To improve solubility, 6 mL of 2-MeTHF was added to the mixture, at which point it became a deep red solution. After 1 h, all volatiles were removed in vacuo. The residue was extracted with 15 mL of diethyl ether and filtered through a plug of Celite. Removal of the diethyl ether in vacuo afforded 160 mg (62% yield) of orange crystalline material. The material was washed generously with pentane and dried in vacuo. NMR parameters for the complex were nearly identical to those of **3** with the exception of a new resonance for the *p*-Me group. <sup>1</sup>H NMR:  $\delta$  74.60 (6 Me<sup>Bn</sup>), 21.97 (2 carbene-CH), 21.57 (4 CHMe<sub>2</sub>), 19.35 (4 *m*-Ar<sup>IPr</sup>H), 12.06 (2 *p*-Ar<sup>IPr</sup>H), −5.97 (12 CHMe<sub>2</sub>), −19.5 (br, 12 CHMe<sub>2</sub>), −42.9 (br, 4 *o*/*m*-Ar<sup>Bn</sup>H), −79.6 (br, 4 *o*/*m*-Ar<sup>Bn</sup>H).

[Fe(*o*-tolyl)<sub>2</sub>(IPr)], **5**. A round-bottom flask was charged with 267 mg (259 μmol) of [Fe<sub>2</sub>Cl<sub>2</sub>(μ-Cl)<sub>2</sub>(IPr)<sub>2</sub>] and 5 mL of 2-MeTHF. The resulting solution was frozen at -196 °C. To the stirring/thawing solution was added 970 μL (1.04 mmol) of *o*-tolylMgCl as a 1.07 M solution in THF. The resulting mixture was stirred for 6 h at ambient temperature and then filtered through a plug of Celite. The solvent volume was reduced in vacuo, and the solution was chilled to -30 °C for 24 h, during which time the desired compound precipitated as off-white crystals. The mother liquor was decanted, and the crystals were washed with pentane and dried in vacuo to afford 133 mg (41% yield). Crystals suitable for X-ray diffraction were grown by vapor diffusion of pentane into a saturated benzene solution. <sup>1</sup>H NMR: δ 223.6 (v br, 2 *o*-Ar<sup>tol</sup>H), 178.17 (2 *m*-Ar<sup>tol</sup>H), 151.40 (2 *m*-Ar<sup>tol</sup>H), 15.97 (4 *m*-Ar<sup>IPr</sup>H), 12.18 (12 CHMe<sub>2</sub>), 10.89 (2 *p*-Ar<sup>IPr</sup>H), -2.1 (v br, 4 CHMe<sub>2</sub>), -5.11 (12 CHMe<sub>2</sub>), -6.47 (2 carbene-CH), -28.3 (br, 6 *Me*-tolyl), -52.46 (2 *p*-Ar<sup>tol</sup>H). Anal. Calcd for C<sub>41</sub>H<sub>50</sub>FeN<sub>2</sub>·1/2C<sub>5</sub>H<sub>12</sub>: C, 78.58; H, 8.52; N, 4.23. Found: C, 78.33; H, 8.80; N, 3.94.

## ■ ASSOCIATED CONTENT

### ● Supporting Information

The Supporting Information is available free of charge on the ACS Publications website at DOI: 10.1021/acscatal.5b01445.

Additional spectra of **3**, **4**, and **5** and mixtures thereof; cyclic voltammogram of **3** in THF; thermal ellipsoid drawings of **5** and **2-I**; crystallographic data and refinement parameters for **5** and **2-I**; and selected bond metrics for **5** and **2-I**. (PDF)

Crystallographic information (CIF)

## ■ AUTHOR INFORMATION

### Corresponding Author

\*E-mail: zachary.tonzetich@utsa.edu.

### Notes

The authors declare no competing financial interest.

## ■ ACKNOWLEDGMENTS

The authors thank the Welch Foundation (AX-1772 to ZJT) for financial support of this work. The CENTC Elemental Analysis Facility is supported by NSF (CHE-0650456).

## ■ REFERENCES

- Bohm, C.; Legros, J.; Le Paih, J.; Zani, L. *Chem. Rev.* **2004**, *104*, 6217–6254.
- Bauer, I.; Knölker, H.-J. *Chem. Rev.* **2015**, *115*, 3170–3387.
- Ingleson, M. J.; Layfield, R. A. *Chem. Commun.* **2012**, *48*, 3579–3589.
- Bézier, D.; Sortais, J.-B.; Darcel, C. *Adv. Synth. Catal.* **2013**, *355*, 19–33.
- Riener, K.; Haslinger, S.; Raba, A.; Högerl, M. P.; Cokoja, M.; Herrmann, W. A.; Kühn, F. E. *Chem. Rev.* **2014**, *114*, 5215–5272.
- Hatakeyama, T.; Nakamura, M. *J. Am. Chem. Soc.* **2007**, *129*, 9844–9845.
- Hatakeyama, T.; Hashimoto, S.; Ishizuka, K.; Nakamura, M. *J. Am. Chem. Soc.* **2009**, *131*, 11949–11963.
- Chua, Y.-Y.; Duong, H. A. *Chem. Commun.* **2014**, *50*, 8424–8427.
- Guisán-Ceinos, M.; Tato, F.; Buñuel, E.; Calle, P.; Cárdenas, D. J. *Chem. Sci.* **2013**, *4*, 1098–1104.
- Bedford, R. B.; Betham, M.; Bruce, D. W.; Danopoulos, A. A.; Frost, R. M.; Hird, M. *J. Org. Chem.* **2006**, *71*, 1104–1110.
- Noda, D.; Sunada, Y.; Hatakeyama, T.; Nakamura, M.; Nagashima, H. *J. Am. Chem. Soc.* **2009**, *131*, 6078–6079.
- Nakamura, M.; Matsuo, K.; Ito, S.; Nakamura, E. *J. Am. Chem. Soc.* **2004**, *126*, 3686–3687.
- Czaplik, W. M.; Mayer, M.; Jacobi von Wangelin, A. *Angew. Chem., Int. Ed.* **2009**, *48*, 607–610.
- Cahiez, G.; Foulgoc, L.; Moyeux, A. *Angew. Chem., Int. Ed.* **2009**, *48*, 2969–2972.
- Hatakeyama, T.; Hashimoto, T.; Kondo, Y.; Fujiwara, Y.; Seike, H.; Takaya, H.; Tamada, Y.; Ono, T.; Nakamura, M. *J. Am. Chem. Soc.* **2010**, *132*, 10674–10676.
- Yamagami, T.; Shintani, R.; Shirakawa, E.; Hayashi, T. *Org. Lett.* **2007**, *9*, 1045–1048.
- Rosa, J. N.; Reddy, R. S.; Candeias, N. R.; Cal, P. M. S. D.; Gois, P. M. P. *Org. Lett.* **2010**, *12*, 2686–2689.
- Lipschutz, M. I.; Chantarojsiri, T.; Dong, Y.; Tilley, T. D. *J. Am. Chem. Soc.* **2015**, *137*, 6366–6372.
- Plietker, B.; Dieskau, A.; Möws, K.; Jatsch, A. *Angew. Chem., Int. Ed.* **2008**, *47*, 198–201.
- Holzwarth, M.; Dieskau, A.; Tabassam, M.; Plietker, B. *Angew. Chem., Int. Ed.* **2009**, *48*, 7251–7255.
- Dieskau, A. P.; Holzwarth, M. S.; Plietker, B. *J. Am. Chem. Soc.* **2012**, *134*, 5048–5051.
- Alt, I.; Rohse, P.; Plietker, B. *ACS Catal.* **2013**, *3*, 3002–3005.
- Kandepi, V. V. K. M.; Cardoso, J. M. S.; Peris, E.; Royo, B. *Organometallics* **2010**, *29*, 2777–2782.
- Jiang, F.; Bézier, D.; Sortais, J.-B.; Darcel, C. *Adv. Synth. Catal.* **2011**, *353*, 239–244.
- Bézier, D.; Venkanna, G. T.; Sortais, J.-B.; Darcel, C. *ChemCatChem* **2011**, *3*, 1747–1750.
- Buitrago, E.; Zani, L.; Adolfsson, H. *Appl. Organomet. Chem.* **2011**, *25*, 748–752.
- Hashimoto, T.; Urban, S.; Hoshino, R.; Ohki, Y.; Tatsumi, K.; Glorius, F. *Organometallics* **2012**, *31*, 4474–4479.
- Buitrago, E.; Tinnis, F.; Adolfsson, H. *Adv. Synth. Catal.* **2012**, *354*, 217–222.
- Misal Castro, L. C.; Sortais, J.-B.; Darcel, C. *Chem. Commun.* **2012**, *48*, 151–153.
- César, V.; Misal Castro, L. C.; Dombay, T.; Sortais, J.-B.; Darcel, C.; Labat, S.; Miqueu, K.; Sotiropoulos, J.-M.; Brousses, R.; Lugan, N.; Lavigne, G. *Organometallics* **2013**, *32*, 4643–4655.
- Louie, J.; Grubbs, R. H. *Chem. Commun.* **2000**, 1479–1480.
- Layfield, R. A.; McDouall, J. J. W.; Scheer, M.; Schwarzmaier, C.; Tuna, F. *Chem. Commun.* **2011**, *47*, 10623–10625.
- Danopoulos, A. A.; Braunstein, P.; Stylianides, N.; Wesolek, M. *Organometallics* **2011**, *30*, 6514–6517.
- Meyer, S.; Orben, C. M.; Demeshko, S.; Dechert, S.; Meyer, F. *Organometallics* **2011**, *30*, 6692–6702.
- Xiang, L.; Xiao, J.; Deng, L. *Organometallics* **2011**, *30*, 2018–2025.
- Raba, A.; Cokoja, M.; Ewald, S.; Riener, K.; Herdtweck, E.; Pöthig, A.; Herrmann, W. A.; Kühn, F. E. *Organometallics* **2012**, *31*, 2793–2800.
- Danopoulos, A. A.; Braunstein, P.; Wesolek, M.; Monakhov, K. Y.; Rabu, P.; Robert, V. *Organometallics* **2012**, *31*, 4102–4105.
- Wu, J.; Dai, W.; Farnaby, J. H.; Hazari, N.; Le Roy, J. J.; Mereacre, V.; Murugesu, M.; Powell, A. K.; Takase, M. K. *Dalton* **2013**, *42*, 7404–7413.
- Warratz, S.; Postigo, L.; Royo, B. *Organometallics* **2013**, *32*, 893–897.
- Hashimoto, T.; Hoshino, R.; Hatanaka, T.; Ohki, Y.; Tatsumi, K. *Organometallics* **2014**, *33*, 921–929.
- Mo, Z.; Ouyang, Z.; Wang, L.; Fillman, K. L.; Neidig, M. L.; Deng, L. *Org. Chem. Front.* **2014**, *1*, 1040–1044.
- Zhang, H.; Ouyang, Z.; Liu, Y.; Zhang, Q.; Wang, L.; Deng, L. *Angew. Chem., Int. Ed.* **2014**, *53*, 8432–8436.
- Day, B. M.; Pugh, T.; Hendriks, D.; Guerra, C. F.; Evans, D. J.; Bickelhaupt, F. M.; Layfield, R. A. *J. Am. Chem. Soc.* **2013**, *135*, 13338–13341.
- Blom, B.; Tan, G.; Enthaler, S.; Inoue, S.; Epping, J. D.; Driess, M. *J. Am. Chem. Soc.* **2013**, *135*, 18108–18120.



- (45) Hopkinson, M. N.; Richter, C.; Schedler, M.; Glorius, F. *Nature* **2014**, *510*, 485–496.
- (46) Przyojski, J. A.; Arman, H. D.; Tonzetich, Z. J. *Organometallics* **2012**, *31*, 3264–3271.
- (47) Liu, Y.; Xiao, J.; Wang, L.; Song, Y.; Deng, L. *Organometallics* **2015**, *34*, 599–605.
- (48) Wang, X.; Zhang, J.; Wang, L.; Deng, L. *Organometallics* **2015**, *34*, 2775–2782.
- (49) Hatakeyama, T.; Fujiwara, Y.-i.; Okada, Y.; Itoh, T.; Hashimoto, T.; Kawamura, S.; Ogata, K.; Takaya, H.; Nakamura, M. *Chem. Lett.* **2011**, *40*, 1030–1032.
- (50) Daifuku, S. L.; Al-Afyouni, M. H.; Snyder, B. E. R.; Kneebone, J. L.; Neidig, M. L. *J. Am. Chem. Soc.* **2014**, *136*, 9132–9143.
- (51) Jin, M.; Adak, L.; Nakamura, M. *J. Am. Chem. Soc.* **2015**, *137*, 7128–7134.
- (52) Adams, C. J.; Bedford, R. B.; Carter, E.; Gower, N. J.; Haddow, M. F.; Harvey, J. N.; Huwe, M.; Cartes, M. À.; Mansell, S. M.; Mendoza, C.; Murphy, D. M.; Neeve, E. C.; Nunn, J. *J. Am. Chem. Soc.* **2012**, *134*, 10333–10336.
- (53) Bedford, R. B.; Carter, E.; Cogswell, P. M.; Gower, N. J.; Haddow, M. F.; Harvey, J. N.; Murphy, D. M.; Neeve, E. C.; Nunn, J. *Angew. Chem., Int. Ed.* **2013**, *52*, 1285–1288.
- (54) Bedford, R. B.; Brenner, P. B.; Carter, E.; Carvell, T. W.; Cogswell, P. M.; Gallagher, T.; Harvey, J. N.; Murphy, D. M.; Neeve, E. C.; Nunn, J.; Pye, D. R. *Chem. - Eur. J.* **2014**, *20*, 7935–7938.
- (55) Bedford, R. B. *Acc. Chem. Res.* **2015**, *48*, 1485–1493.
- (56) Bauer, G.; Wodrich, M. D.; Scopelliti, R.; Hu, X. *Organometallics* **2015**, *34*, 289–298.
- (57) Czaplik, W. M.; Mayer, M.; Cvengros, J.; von Wangelin, A. *J. ChemSusChem* **2009**, *2*, 396–417.
- (58) Kleimark, J.; Hedström, A.; Larsson, P.-F.; Johansson, C.; Norrby, P.-O. *ChemCatChem* **2009**, *1*, 152–161.
- (59) Hedström, A.; Bollmann, U.; Bravidor, J.; Norrby, P.-O. *Chem. - Eur. J.* **2011**, *17*, 11991–11993.
- (60) Kleimark, J.; Larsson, P.-F.; Emamy, P.; Hedström, A.; Norrby, P.-O. *Adv. Synth. Catal.* **2012**, *354*, 448–456.
- (61) Schoch, R.; Desens, W.; Werner, T.; Bauer, M. *Chem. - Eur. J.* **2013**, *19*, 15816–15821.
- (62) Lefèvre, G.; Jutand, A. *Chem. - Eur. J.* **2014**, *20*, 4796–4805.
- (63) Bekhradnia, A.; Norrby, P.-O. *Dalton* **2015**, *44*, 3959–3962.
- (64) Hedström, A.; Izakian, Z.; Vreto, I.; Wallentin, C.-J.; Norrby, P.-O. *Chem. - Eur. J.* **2015**, *21*, 5946–5953.
- (65) Fürstner, A.; Leitner, A. *Angew. Chem., Int. Ed.* **2002**, *41*, 609–612.
- (66) Bedford, R. B.; Bruce, D. W.; Frost, R. M.; Hird, M. *Chem. Commun.* **2005**, 4161–4163.
- (67) Gao, H.-H.; Yan, C.-H.; Tao, X.-P.; Xia, Y.; Sun, H.-M.; Shen, Q.; Zhang, Y. *Organometallics* **2010**, *29*, 4189–4192.
- (68) Deng, H.-n.; Xing, Y.-l.; Xia, C.-l.; Sun, H.-m.; Shen, Q.; Zhang, Y. *Dalton* **2012**, *41*, 11597–11607.
- (69) Mo, Z.; Zhang, Q.; Deng, L. *Organometallics* **2012**, *31*, 6518–6521.
- (70) Ghorai, S. K.; Jin, M.; Hatakeyama, T.; Nakamura, M. *Org. Lett.* **2012**, *14*, 1066–1069.
- (71) Okada, S.; Park, S.; Matyjaszewski, K. *ACS Macro Lett.* **2014**, *3*, 944–947.
- (72) Poli, R.; Shaver, M. P. *Inorg. Chem.* **2014**, *53*, 7580–7590.
- (73) Xue, Z.; He, D.; Xie, X. *Polym. Chem.* **2015**, *6*, 1660–1687.
- (74) Loginova, K. A.; Knyazev, V. D. *J. Phys. Chem. A* **2011**, *115*, 8616–8622.
- (75) Musgrave, R. A.; Turbervill, R. S. P.; Irwin, M.; Herchel, R.; Goicoechea, J. M. *Dalton* **2014**, *43*, 4335–4344.
- (76) Fillman, K. L.; Przyojski, J. A.; Al-Afyouni, M. H.; Tonzetich, Z. J.; Neidig, M. L. *Chem. Sci.* **2015**, *6*, 1178–1188.
- (77) Bedford, R. B.; Brenner, P. B.; Carter, E.; Cogswell, P. M.; Haddow, M. F.; Harvey, J. N.; Murphy, D. M.; Nunn, J.; Woodall, C. H. *Angew. Chem., Int. Ed.* **2014**, *53*, 1804–1808.
- (78) Bedford, R. B.; Huwe, M.; Wilkinson, M. C. *Chem. Commun.* **2009**, 600–602.
- (79) Daifuku, S. L.; Kneebone, J. L.; Snyder, B. E. R.; Neidig, M. L. *J. Am. Chem. Soc.* **2015**, [10.1021/jacs.5b06648](https://doi.org/10.1021/jacs.5b06648).
- (80) Dunsford, J. J.; Cade, I. A.; Fillman, K. L.; Neidig, M. L.; Ingleson, M. J. *Organometallics* **2014**, *33*, 370–377.
- (81) Liu, Y.; Luo, L.; Xiao, J.; Wang, L.; Song, Y.; Qu, J.; Luo, Y.; Deng, L. *Inorg. Chem.* **2015**, *54*, 4752–4760.
- (82) Sherry, B. D.; Fürstner, A. *Acc. Chem. Res.* **2008**, *41*, 1500–1511.
- (83) Johnson, S. A.; Kiernicki, J. J.; Fanwick, P. E.; Bart, S. C. *Organometallics* **2015**, *34*, 2889–2895.
- (84) Schlosser, M.; Hartmann, J. *Angew. Chem., Int. Ed. Engl.* **1973**, *12*, 508–509.
- (85) *Crystal Clear*; Rigaku/MSI Inc.; Rigaku Corporation: The Woodlands, TX, 2005.
- (86) ABSCOR; Higashi; Rigaku Corporation: Tokyo, Japan, 1995.
- (87) Sheldrick, G. M. *SHELXTL97: Program for Refinement of Crystal Structures*; University of Göttingen: Göttingen, Germany, 1997.
- (88) Sheldrick, G. M. *Acta Crystallogr., Sect. A: Found. Crystallogr.* **2008**, *A64*, 112–122.